6th CanSmart Workshop

SMART MATERIALS AND STRUCTURES

16 - 17 October 2003, Montreal, Quebec, Canada.

DESIGN TOOLS FOR PIEZOELECTRIC ACTUATED INCHWORM POSITIONERS

S. SALISBURY[1], D. WAECHTER[2], R. BEN MRAD[1], R. BLACOW[2] AND E. PRASAD[2]

[1]*Department of Mechanical and Industrial Engineering*
5 King's College Road, University of Toronto, ON M5S 3G8

[2]*Sensor Technology Limited*
P.O. Box 97, Collingwood, ON L9Y 3Z4

ABSTRACT

Several piezoactuated inchworm motors are being developed for ultraprecision applications. Performance of the motor depends on the interaction of the frame stiffness and piezoelectric properties. In an effort to develop optimum designs, a set of design equations were derived from standardized kinematic models. They facilitate quick iteration and convergence to an acceptable design based on the requirements. The accuracy of the equations was assessed by comparing them to several finite element analyses. Future research will include prototype tests to validate both the analytical and finite element models.

1. INTRODUCTION

Piezoactuator driven inchworm motors are being developed for applications which require accuracy in the range of nanometres while still having a range of centimetres. Industries such as semiconductor manufacture, photonics and laser machining have such requirements.

In order to more efficiently design such motors, the objective of this work is to develop a set of design tools that can be used in a spreadsheet application to quickly iterate designs. In this way the design can be optimized before lengthy finite element analyses (FEA) or prototype tests are conducted.

2. INCHWORM CONFIGURATION

The design configuration presented in [1,2] (see Fig.1) was used as a basis for the design equations. The left clamping section is fixed while the right section moves due to the extension piezostack. By coordinating the clamping and extension piezostacks in the proper sequence, the moving member can be moved an integral number of steps. The step size is determined by the voltage amplitude applied to the extension piezo. In this manner, the inchworm can use the micro motions of the extension piezo to move macro distances.

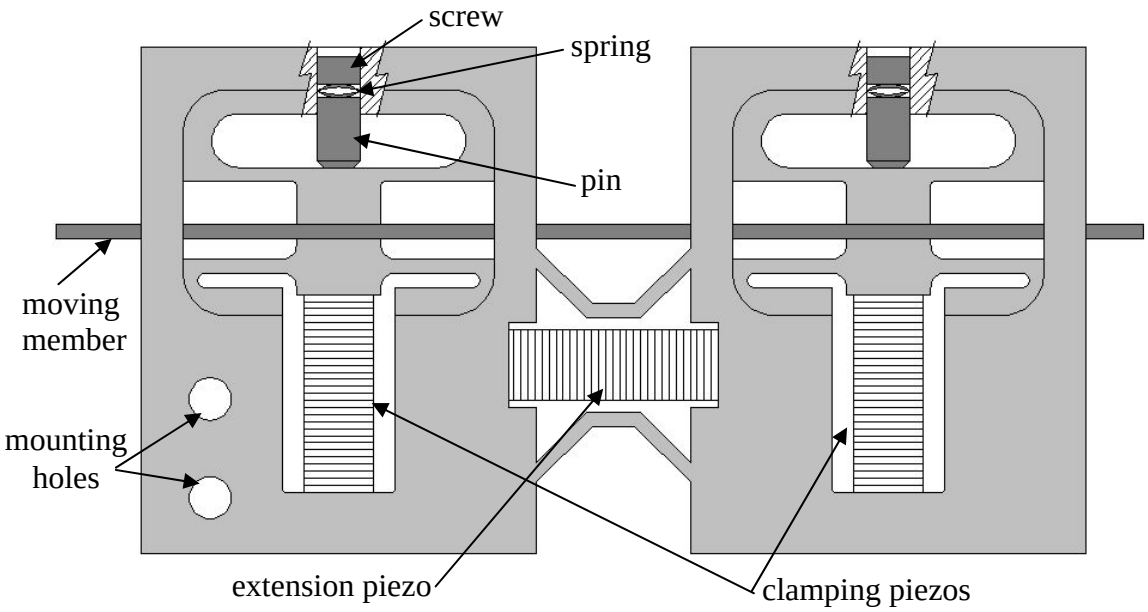

Figure 1: Inchworm Configuration [1,2]

This configuration has an adjustment mechanism to vary the gap between the clamping surfaces in order to account for wear and tolerances. When the piezostack is installed in the clamps, there is a slight interference fit in order to preload the piezostack. This protects it from experiencing tensile forces which degrade the piezostack life.

3. DEVELOPMENT OF CLAMP DESIGN EQUATIONS

The system is analyzed in four different states; before assembly, preloaded, maximum stroke and clamped (see Fig. 2).

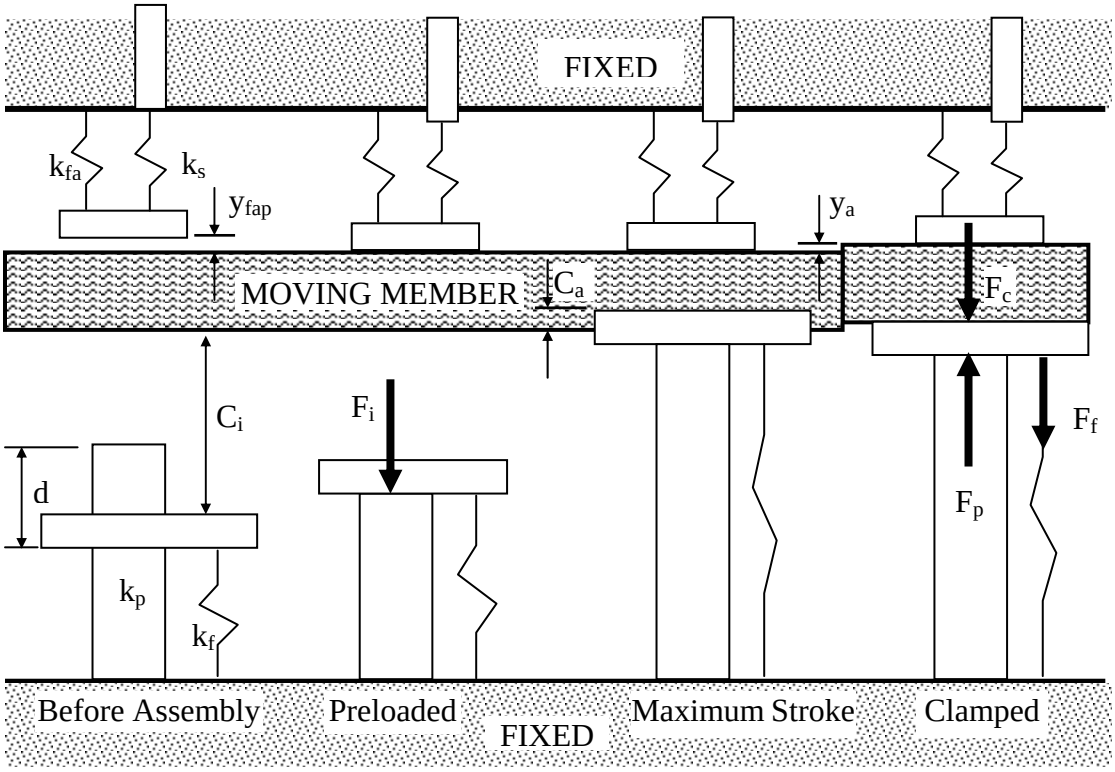

Figure 2: Various States of Clamping [3]

Before assembly, the compliant components are in their free or unloaded state. The piezostack, disc spring, the preload flexure and adjustment flexure have stiffnesses k_p, k_s, k_f and k_{fa} respectively. The flexure has an interference, d, with the piezostack and clearance, C_i, to the moving member. The distance y_{fap} is the amount by which the adjusting flexure will be preloaded in order to set the desired clearance C_i.

In the preload condition, the piezostack is inserted into the flexure cavity and the components will deflect until the length of the piezostack is the same as the flexure cavity. The preload, F_i, on the piezostack can then be solved for to get:

$$F_i = \frac{k_p k_f d}{k_p + k_f} \tag{1}$$

The maximum stroke is the range the piezostack could move while preloaded if the moving member did not restrain its motion. This is important in order to determine the range the clamp will be able to cover. As well, this will determine the clamping force in the next stage. The clamping allowance, C_a, is the amount of stroke which is in excess of the remaining distance to the moving member. The greater the allowance, the more the clamping force will be. C_a is found to be:

$$C_a = \frac{k_p(L_o + d)}{k_p + k_f} - C_i \tag{2}$$

For the clamped condition, the clamping force, F_c, counteracts the piezostack to stop the extension at the moving member. The clamping force causes a slight deflection of the adjustment mechanism which must also be accounted for. Solving for this deflection, y_a, gives:

$$y_a = \frac{(d - C_i + L_o)\cdot k_p - C_i \cdot k_f}{k_p + k_f + k_{fa} + k_s} \tag{3}$$

Now F_p, F_f and F_c can be determined based on y_a:

$$F_c = (k_s + k_{fa})\cdot y_a \tag{4}$$

$$F_f = k_f(C_i + y_a) \tag{5}$$

$$F_p = -F_f - F_c \tag{6}$$

The forces on the components can be used to evaluate their stress levels and margins of safety.

3.1 Flexure Model

While the above equations were developed for a particular configuration, the flexures used in the clamping sections are found in several designs, so a generalized flexure design is modelled. The model was developed based on a pair of straight flexures with corner radii (see Fig. 3). Due to symmetry, the flexure can be modelled as a cantilever beam with point load and an end moment (see Fig. 4). The stiffness calculation does not account for the corner radii but they are included in the stress calculation. The margins of safety are calculated based on the fatigue strength of the flexure material. Fatigue will be the dominant mode since several steps are needed to move a significant distance.

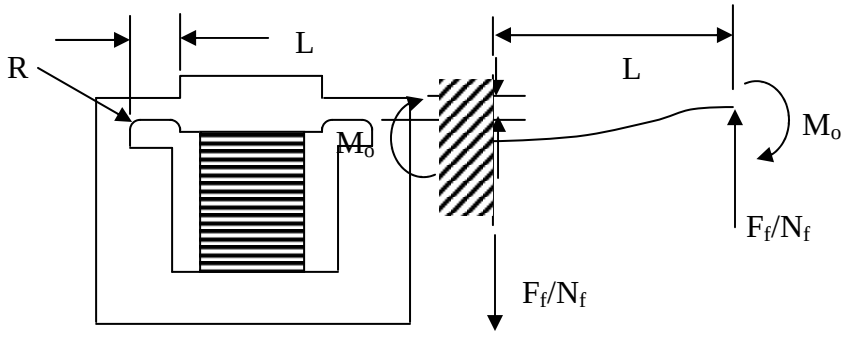

Figure 3: Dimensions of Flexure **Figure 4: Flexure Beam Model**

The total stiffness of the flexure is calculated by rearranging the equation for the deflection given in [4]:

$$k_f = N_f \frac{Ew(t/L)^3}{1+2C(1+\nu)(t/L)^2} \tag{7}$$

where: N_f – number of flexures L – flexure length
w – flexure width t – flexure thickness
E – modulus of elasticity ν - Poisson's ratio
C – shear stress correction factor (=1.50 for rectangular beams)

The stiffness is composed of both bending and shear stress effects. Normally shear effects are ignored, however for short beams the effects are significant as will be shown in the FEA section [5].

To ensure that the flexure will not fracture the bending stress, σ_b, can be determined for the flexure [5].

$$\sigma_b = K \frac{3F_f L}{N_f wt^2} \tag{8}$$

The factor, *K*, is the stress concentration factor and is determined based on the relative size of the radius compared to the flexure thickness [5]. Using the fatigue strength of the material, the safety margin is calculated to ensure that the design will function adequately over its lifespan.

4. COMPARISON OF FLEXURE MODEL TO FINITE ELEMENT ANALYSIS

There are several variables in the design, however the width and length are usually constrained by physical limits in the design while the thickness can be varied. For this reason the FEA study of the flexure examines the effect of thickness on stiffness [6]. The other parameters are fixed at values common in many inchworm designs.

The FEA model is shown in Fig. 6. The bottom edge is fixed and the lower structure is removed as it contributes little to the stiffness. The right edge has a symmetry condition and a pressure load is applied in the area where the piezo would contact the flexure. The material is chosen as hardened stainless steel with the following properties; E = 200 GPa, ν = 0.27.

A typical result for the stress distribution is shown in Fig. 6. The highest stress concentration is at the two support points. The vertical deflection of the piezo contact surface is measured and the stiffness calculated for a range of thicknesses. The graph in Fig. 7 shows the comparison of the analytically determined stiffness and stress as compared to the FEA results. It can be seen that for thickness values less than 1.0 mm, the stiffness calculations agree quite well. However, above 1.0 mm, the calculation

difference increases rapidly. The difference between the analytical and FEA stiffness is due to the end effects which are not accounted for in the analytical model. If the calculation for stiffness includes shear effects then the error is not as large, which is the reason it is included in the analytical calculation.

The analytical stress calculation approaches the FEA stress as the thickness increases. Since the analytical stress overestimates the FEA, the analytical method will have a higher margin of safety than the FEA.

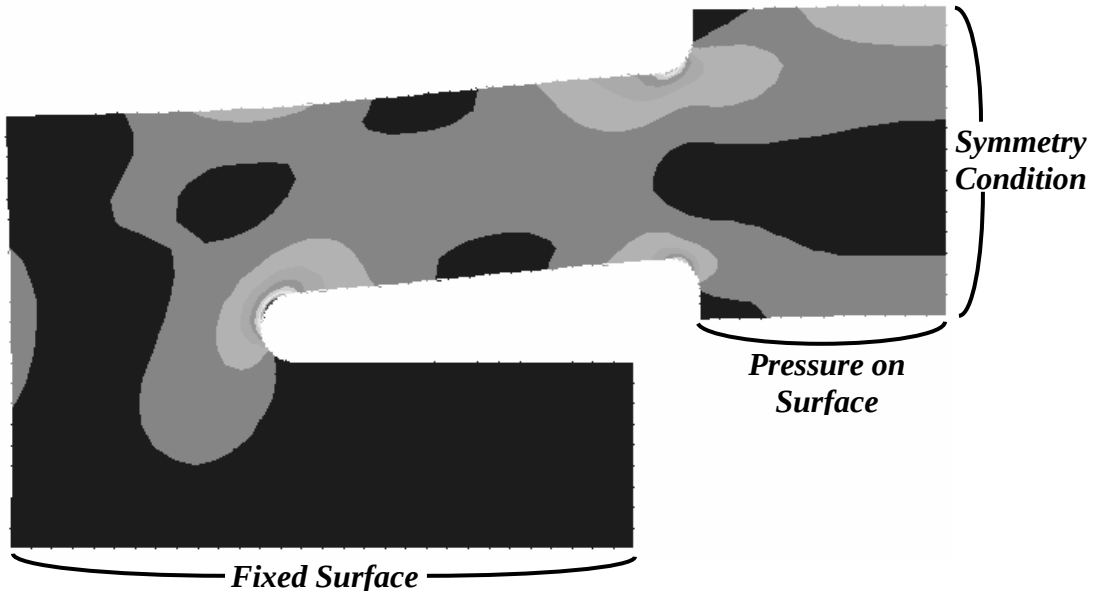

Figure 5: FEA von Mises Stress Distribution [6]

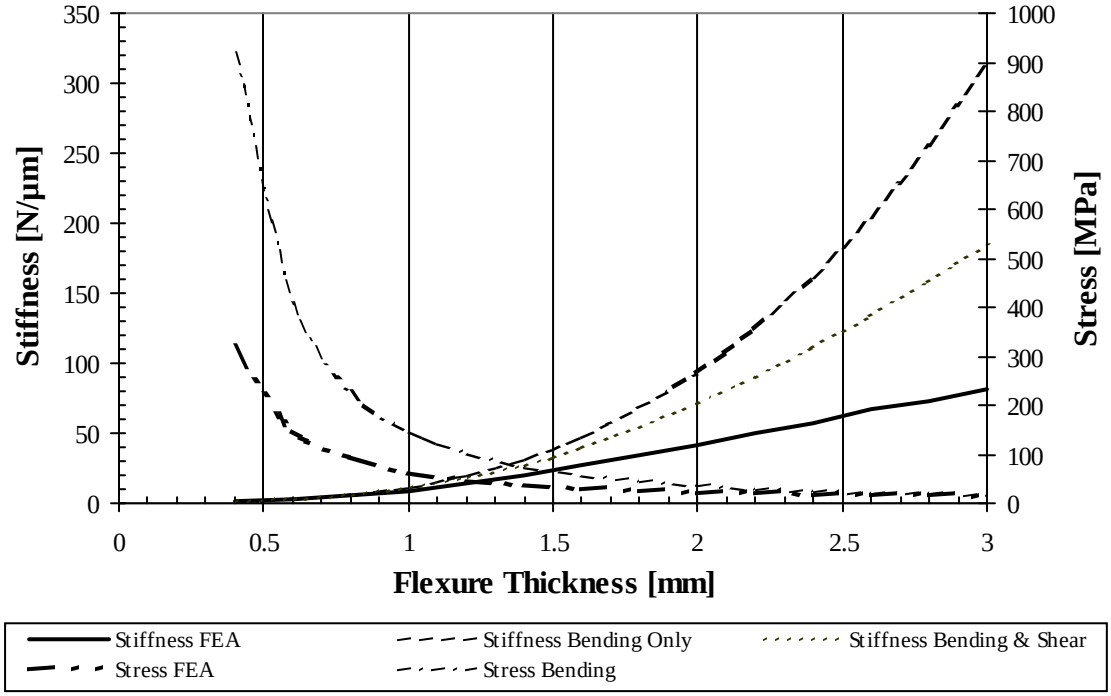

Figure 6: Analytical and FEA Comparison [6]

5. CONCLUSIONS

An analytical method for iterative clamp design was developed. The stiffness and stress of the analytical flexure model was compared to those determined from an FEA model. The analytical stiffness departs from the FEA stiffness as the thickness increases. However, closer results are obtained if shear effects are included in the calculation. The analytical stress overestimated the FEA stress which will result in higher margins of safety. Future research will include prototype tests to validate both the analytical and finite element models.

6. REFERENCES

[1] D. Waechter, High Displacement High Force Piezoelectric Actuator for Shape Control of Space and Terrestrial Systems, Collingwood: Sensor Technology Limited, Technical Report, 2002.

[2] D. Waechter, Clamp Section Cavity Design Concept for Precision Fit of Stack Actuator, Collingwood: Sensor Technology Limited, Technical Report, Feb. 2003.

[3] S. Salisbury and R. Ben Mrad, Design Tools for an Inchworm Positioner, Toronto: University of Toronto, Technical Report, Jan. 2003.

[4] E. Oberg, F. Jones, H. Horton and H. Ryffel, Machinery's Handbook 25th Edition, New York: Industrical Press Inc., 1996.

[5] J. Shigley and C. Mischke, Mechanical Engineering Design, 5th ed. , New York: McGraw-Hill, 1989.

[6] S. Salisbury and R. Ben Mrad, Inchworm Positioner FEA Analysis, Toronto: University of Toronto, Technical Report, Jun. 2003.